# Characterization of Petrophysical Properties of Reservoirs in Bima Formation, Northeastern Nigeria: Implication for Hydrocarbon Exploration

[1]Omolaiye , G.E., [2]Ajadi, J., [3]Saminu, O., [2]Jimoh, Y.A. and [4]Daniel U.

[1]Geoslice Solution Limited, Lagos Nigeria.
[2] Department of Geology and Mineral Science, Kwara State University, Malete,, Nigeria
[3]Department of Geophysics, University of Ilorin, Nigeria
[4]Guarantee Petroleum Limited, Lagos Nigeria

## ABSTRACT

Characterization of petrophysical properties of reservoirs in Bima Formation was undertaken to understand their spatial distribution and impacts on hydrocarbon saturation in the highly heterolithic siliciclastic sequence. The study was carried out using nine well logs from Maiduguri and Baga/Lake sub-basins within the Borno Basin. Evaluation of the formation reveals largely undifferentiated to highly serrated and lenticular sand bifurcated by shale beds, which reduced their thicknesses variably from 0.61 to 6.1 m. The shale content in the sand bodies ranged from 11.00% to 88.00%. The formation also has variable porosity values, with calculated total porosity ranged from 10.00% to 35.00%. Similarly, effective porosity values spanned between 2.00 to 24.00%. The irregular porosity values also accounted for a wide range of field average permeability estimates computed for the formation, which measured between 0.03 to 319.49mD. Hydrocarbon saturation also varied from 40.00 to 78.00%. Gas accumulation was encountered in Ga-1, Da-1, Ar-1 and Ye-1 wells. These highly thin serrated sand beds with variable porosity and permeability constitute exploration challenges. The very thinly laminated or serrated alternation of sand and shale beds lithofacies of the Bima Formation is supportive of fluvio-lacustrine depositional environments.

**Key words: Bima, Chad Basin, fluvio-lacustrine, lithofacies and serrated sand**

## Introduction

The search for hydrocarbon in the northern frontier basins of Nigeria receives renewed prime attention of recent, based on the need to increase hydrocarbon reserves. Chad basin in particular has continued to draw intense exploration interest over half a century, sequel to successes recorded in the geologically contiguous segments of the Republic of Chad, Niger, Cameroun and Southern Sudan. The drive engendered diverse research curiosity including studies of depositional and structural style (Avbovbo *et al.*, 1986), geochemical analysis of source-rock (Olugbenro *et al.*, 1997; Boboye & Abimbola 2009; Alalade & Tyson 2010), reservoir characterization (Adepelumi *et al.,* 2011), provenance and paleoenvironment (Haruna *et al.,* 2013) and depositional environment (Obiora *et al.,* 2014). Haruna *et al.,* (2013) traced the source sediments to Adamawa, Cameroun, Mandara and Hawal Massifs.

GALLEY PROOF

They also inferred that Bima sandstone was deposited during tectonic quiescence in humid tropical climate in the Mid-Cretaceous times. Furthermore, Obiora *et al.,* (2014) analyzed 15 samples from part of the basin and revealed that the depositional energy of the environment ranges from medium to high, while the sediments are positively skewed, suggesting river sand, with sorting mean deviation ranges from 0.87 to 1.75, reflecting poor to moderately sorted sand. They also interpreted fluviatile origin for the sediment based on bivariate plot of skewness versus sorting and mean grain size versus sorting. The lithofacies associations of Bima sand was studied to deduce the nature of the depositional environment and it was noted that facies distribution represents a basinward change in depositional environments from marginal alluvial fan to axial lacustrine system (Opeloye, 2012). The author identified four lithofacies association (FA I to FA IV) based on lithology, grain size and sedimentary structure. Besides, seismic and petrophysical investigation of the basin also drew the attention of many workers.

The importance of petrophysical characterization of petroleum system has long been recognized. For instance, some hydrocarbon resource may be bypassed or remained unproduced after discovery and exploitation partly due to dearth of understanding of the reservoir properties or the available technology. Larue and Legarre (2004) noted that data paucity, time limitation, model building and model resolution make reservoir characterization inadequate to represent actual geologic variability of sand. The primary focus of this study is to characterize and evaluate the petrophysical properties of Bima sand in Maiduguri and Baga /lake sub-basins of Borno basin in order to understand its intrinsic petrophysical properties, such as shale volume distribution, porosity, water saturation, permeability and hydrocarbon saturation.

**Geology and Structural Framework of Chad Basin**

The Chad basin is one of the largest basins in Central African region. This intracratonic basin has geographical spread that cuts across Niger Republic, Nigeria, Chad and Cameroun, an area that remain relatively quiescent geologically over a long period. A five-phased tectonic history dating from the Pan African orogeny to the present suggests that Chad basin (Fig. 1), a component of West African Rift System (WAS), which was formed mainly by the mechanical separation of African crustal blocks during Early Cretaceous, is extensional in characteristics with thick continental to marine clastics sediments and minor volcanics (Genik, 1992). Thick deposit of predominantly siliciclastic sedimentary layers, in addition to the discovery of commercial quantity of hydrocarbon in neighboring countries within the basin, accentuates exploration interest in the Nigerian segments.

GALLEY PROOF

**Stratigraphic Setting of the Chad basin**

The Borno basin consists of marine to fluviatile/deltaic sediments. The stratigraphic framework of the basin comprises of the following lithostratigraphic units from bottom to top, viz-a-viz: the Pre-Bima, Bima, Gongila, Fika, Gombe, Kerri-Kerri and Chad Formations (Avbovbo *et al.,* 1986).

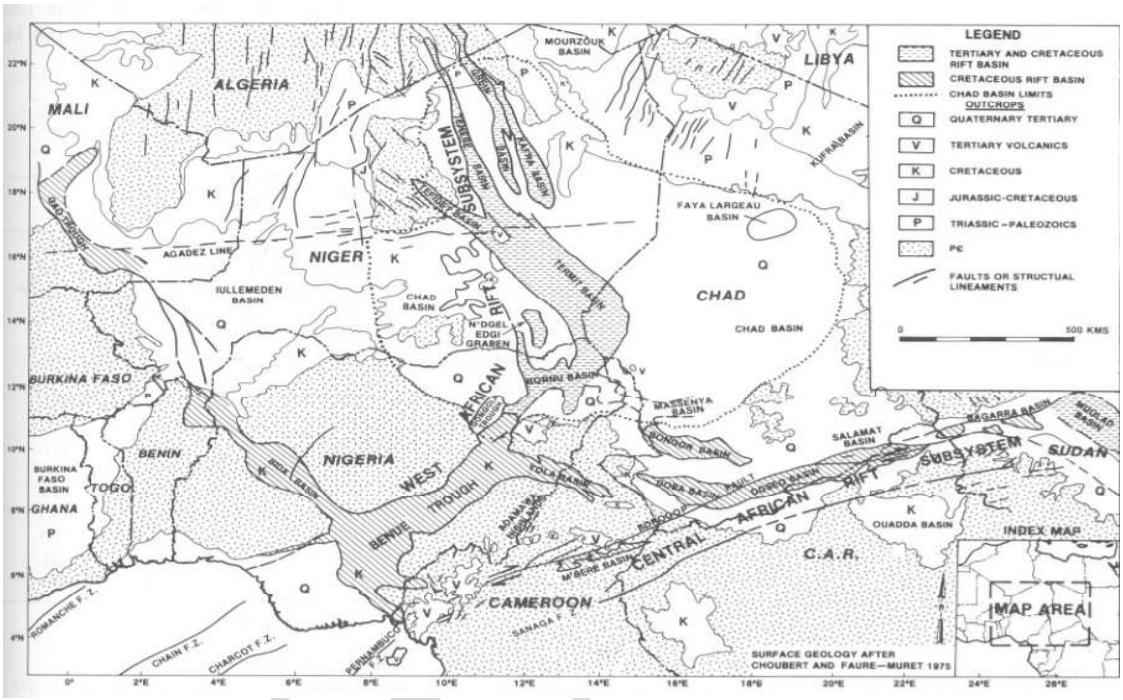



Figure 1: Regional map with rifts superposed upon the regional surface geology, showing the position of the West African rift subsystem (Genik, 1992).

**MATERIALS AND METHODS**

This study was based on detailed analysis of nine wells from Maiduguri Area and Baga/Lake Area in the Southwest and Northeast respectively within the Chad Basin (Fig. 2). The available wells used from Maiduguri Area include: Na-1, Ga-1, Ar-1, Di-1 and Ye-1, while in Baga/Lake Area were Sa-1, Te-1, Da-1 and Wa-1. The wells comprise of key log curves, namely: gamma ray, resistivity, sonic, bulk density and neutron porosity (Table 1).

The well logs were relatively of good quality. However, minimal corrections were done to eliminate borehole effects, while intervals with abnormal curves were patched. The top and base of each Formation, as interpreted from high resolution biostratigraphic study were posted on the well logs to facilitate interwells correlation. The base of Chad Formation was picked across the wells and used as a regional bench mark for subsequent correlations of the

deeper Bima Formation within each of the sub basins. The tops and bases of each sand body within the Bima Formation were systematically picked and correlated from one well to the other. Gamma ray log was used to determine lithology and bed boundaries in combination with resistivity, neutron and density logs in discrete intervals. This was followed by correlations and construction of stratigraphic cross sections. Petrophysical properties were studied using a combination of the log curves. Petrophysical properties mainly; porosity, bulk volume water, shale volume, water saturation, hydrocarbon saturation and permeability were calculated from the log data.

Table 1: Chad Basin Well Log Inventory showing the key curves used for this work

| Well Data Inventory | | | | | | | | |
|---|---|---|---|---|---|---|---|---|
| S/NO | WELL | CALI | SP | Gamma Ray | Resistivity | RHOB | NPHI | Sonic |
| | | | | | | | | |
| 1 | Te-1 | – | λ | λ | λ | λ | λ | λ |
| 2 | Ga-1 | λ | – | λ | λ | λ | λ | λ |
| 3 | Wa-1 | λ | – | λ | λ | λ | λ | λ |
| 4 | Da-1 | λ | – | λ | λ | λ | λ | λ |
| 5 | Na-1 | λ | λ | λ | λ | λ | λ | λ |
| 6 | Sa-1 | λ | λ | λ | λ | λ | λ | λ |
| 7 | Ar-1 | λ | λ | λ | λ | λ | λ | λ |
| 8 | Di-1 | λ | – | λ | λ | λ | λ | λ |
| 9 | Ye-1 | λ | λ | λ | λ | λ | λ | λ |

*CALI - Caliper, RHOB - Bulk density, NPHI - Neutron pulse hydrogen index

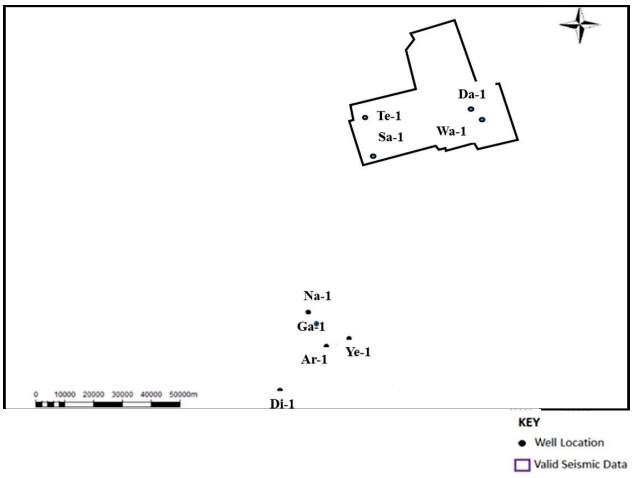



Figure 2: Base map of the study area: Maiduguri and Baga/Lake Sub-basins of the Chad Basin

**Theoretical Basis of Petrophysical Analysis**

***$V_{sh}$ Determination***

Gamma ray log was available in the nine (9) wells studied and was used for shale volume correction. Gamma ray log values were first applied to calculate Gamma Ray Index ( $I_{GR}$ ), a very essential step, because $I_{GR}$ is independent of clay types and this was estimated as follows;

$$I_{GR} = \frac{GR_{log} - GR_{min}}{GR_{max} - GR_{min}} \quad 1$$

Where $I_{GR}$ is the gamma ray index, $GR_{\log}$ is the actual gamma value for the formation at a given depth, $GR_{\min}$ is the minimum gamma ray or cleanest sand reading and $GR_{\max}$ is the maximum gamma ray or shaliest reading. The Steiber volume correction method was examined for use in this study (Steiber, 1970) and the equation is given as:

$$V_{sh} = \frac{I_{GR}}{3.2 * I_{GR}} \quad 2$$

where $V_{sh}$ is the shale volume and $I_{GR}$ is the gamma ray index. The total porosity versus shale volume and gamma ray plots were used to delineate Vsh cut off (Figs. 3 and 4). A plot of DT versus GR (Fig. 6) allows the determination of the ranges for occurrence of clean sand and shale in the formation.

**Formation Water Resistivity**

Formation Water resistivity is a key parameter in petrophysical evaluations. It was observed that resistivity reading in the area is generally high, as interpreted from log values. The Pickett plot approached was adopted to generate formation water resistivity values from relatively clean sand in wet intervals.

Other than Pickett plots, formation water resistivity values can also be obtained mathematically using Archie's (1942) equation. This approach is often employed in water bearing zones, for instance;

GALLEY PROOF

$$R_{wa} = \frac{R_o}{F} \quad (3)$$

The formation resistivity factor is calculated using the Humble formula, given thus;

$$F - \frac{a}{\emptyset^m} \quad (4)$$

Where: $R_o$ = Resistivity at 100% water saturation, F = Formation resistivity factor

$\phi$ = Porosity, m = Cementation factor taken as 2 in this study, a = Tortuosity and

$R_{wa}$ = Apparent formation water resistivity.

**Water Saturation Calculation**

The (Archie, 1942) water saturation was determined from rock resistivity $R_o$ and the true resistivity, $R_t$ Thus:

$$S_w = \left[\frac{R_o}{R_t}\right]^{\frac{1}{n}} \quad (5)$$

A refined form of Archie, 1942 was derived by replacing $R_o$ in equation (5) by $F \times R_w$, so that it becomes;

$$S_w^n - \frac{F * R_w}{R_t} \quad (6)$$

The general form of the (Archie, 1942) equation is given as equation 7, thus;

$$S_w \left[\frac{a * R_w}{R_t * \emptyset^m}\right]^{\frac{1}{n}} \quad (7)$$

where $S_w$ is the connate water saturation, $R_w$ is the formation water resistivity, $R_t$ is the true formation resistivity, m is the cementation factor and n is the saturation exponent, both were assigned the value of 2 respectively in this work, 'a' is tortousity and taken as 1, while $\phi$ is the log derived porosity.

**The Dual Water Method**

Besides the Archie (1942) water saturation approach, the dual water saturation method was examined and used. Bowers and Fitz, (2000) presented an analytic approach to estimate uncertainty in dual water saturation model. A simplified dual-water-model equation is stated thus;

$$S_w T = Y + \sqrt{\left\{\frac{R_W}{\langle [R_t * \emptyset^2] + Y^2 \rangle}\right\}} \quad (8)$$

Where Y is given by;

$$Y = V_{shl} * \left\{\frac{[R_w B_{nd} - R_w]}{[2 * R_w B_{nd}]}\right\} \quad 9$$

Where $S_w T$is the total water saturation, $R_t$ is the true or deep resistivity, $B_{nd}$ is the bond water resistivity, taken as 15 ohms, $R_w$ is the formation water resistivity and $V_{shl}$ is shale volume.

**Permeability Model**

Permeability is a measure of the ease with which fluid flows through interconnected pore spaces of the reservoir rock. In this study, two empirical permeability models namely; Tixier (1949) and Timur (1968) were used for the purpose of comparison.

Tixier (1949) formulated an empirical approach seven years after Archie (1942) to determine permeability from resistivity gradient, based on relation between resistivity and water saturation, water saturation and capillary pressure, and capillary pressure and permeability thus;

$$K = c\left[a\frac{2.3}{\rho_w - \rho_o}\right]^2 \quad 10$$

Where:

$$a = \frac{\Delta R}{\Delta D}\frac{1}{R_o} \quad 11$$

where c is a constant, taken to be 20, $\Delta R$ is the change in resistivity in ohm-m, $\Delta D$ is the change in depth (ft.), corresponding to $\Delta R$, $\rho_w$ is formation water density (g/cm$^3$), $\rho_o$is formation fluid density (g/cm$^3$) and $R_o$is the formation rock matrix resistivity. Combining equations 10 and 11 give;

$$\left[\frac{k}{20}\right]^{\frac{1}{2}} = \frac{2.3}{R_o[d_w - d_o]}\frac{\Delta R}{\Delta D} \quad 12$$

where $\frac{\Delta R}{\Delta D}$ is the resistivity gradient and is determined from resistivity log after effecting correction. Tixier (1949) further modified his equations to a simpler form, as given thus;

$$k^{\frac{1}{2}} = 250\frac{\emptyset^3}{S_{wi}} \quad 13$$

where $S_{wi}$ is the irreducible water saturation.

Timur (1968) later worked on (Kozen, 1927) permeability equation and gave an expression thus;

GALLEY PROOF

$$k = 0.136\frac{\emptyset^{4.4}}{S_{wi}^2} \quad 14$$

In order to derive irreducible water saturation $S_{wi}$, he used the equation;

$$S_{wi} = 3.5\,\frac{\emptyset^{1.26}}{k^{0.35}} - 1 \quad 15$$

This equation assumes a standard error of 13% pore volume and secondly, $S_{wi}$ and $\phi$ are expressed as percentages. Timur (1968) equation is useful where there is residual water saturation and assumes a standard value of 1.5 for cementation factor.

## RESULTS AND DISCUSSION

### Well Interpretation

The shale volume ($V_{shl}$) cutoffs determined for the Bima Formation using two wells; Te-1 and Sa-1 range were very close, $V_{shl}$ 0.76 and $V_{shl}$ 0.80 respectively (Figs. 3 & 4). Similarly, the total porosity (PHIA) cutoffs derived from crossplots of PHIA/ $V_{shl}$ /GR for the entire Te-1 and Sa-1 wells yielded PHIA values of PHIA 0.15 and PHIA 0.16 respectively (Figs. 3 & 4).

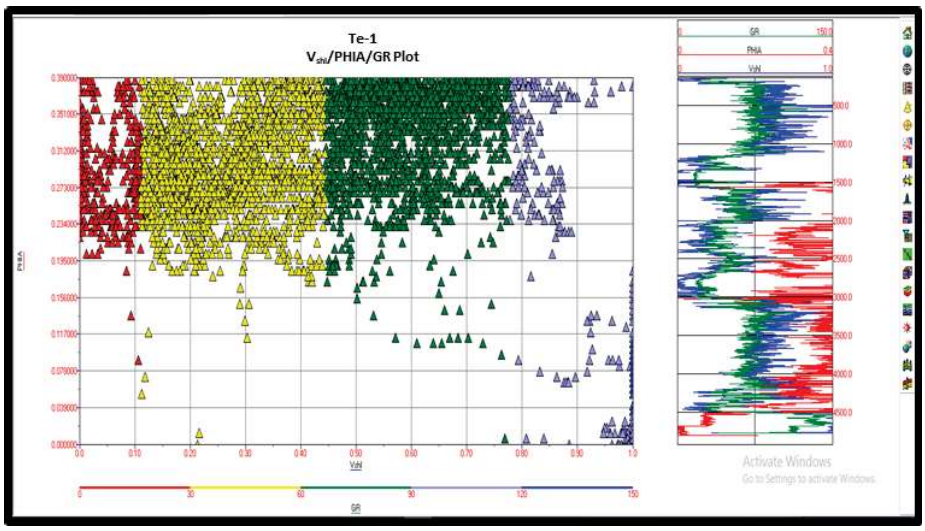



Figure 3: Crossplot for the entire Te-1 Well PHIA/ $V_{shl}$/GR Cutoff: PHIA is 0.15, $V_{shl}$: 0.76

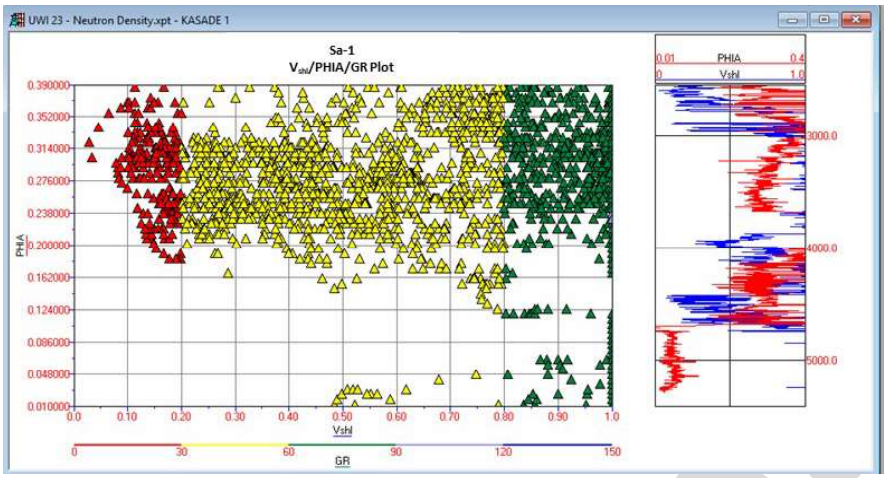



Figure 4: Crossplot for the entire Sa-1 well PHIA/ $V_{shl}$ /GR Cutoff: PHIA is 0.16, $V_{shl}$: 0.80

A plot of DT versus GR (Fig. 5) yielded clean sand Interludes within DT 40 to 100 interval transit time and GR 15 to 64 API, while shale intervals occur at GR values above 64 API.

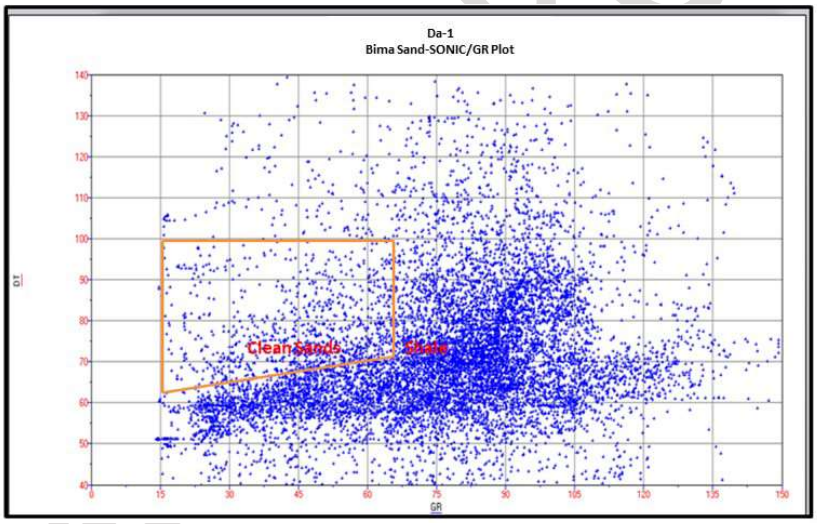



Figure 5: Bima Sand Sonic/GR Plot, Showing Clean Sand Occurring in Da-1 well

Formation water resistivity ($R_w$) values from Pickett Plots were obtained from two wells Wa-1 and Sa-1 within Kerri-Kerri Sand-2 and Kerri-Kerri-1 sand respectively (Figs. 6 and 7). In Wa-1 Well, Kerri-Kerri Sand-2 yielded formation water resistivity value of 0.60299 Ωm. Whereas, in Sa-1 Well the value of formation water resistivity is 1.841Ωm in Kerri-Kerri Sand-1. Due to the highly serrated and shaly nature of Bima Sand; interbedded thin shale beds alternating with thin sand layers, Pickett plots from the sand was deemed unreliable. Hence, formation water resistivity value ($R_w$ 1.841Ωm) from shallower Kerri-Kerri Formation, was used for petrophysical calculations. Anomalously high resistivity log

readings recorded in the field is attributed to mineralization, diagenesis and high ambient formation water resistivity value. This is probably responsible for difficulties encountered by previous workers in reasonably defining hydrocarbon saturation.

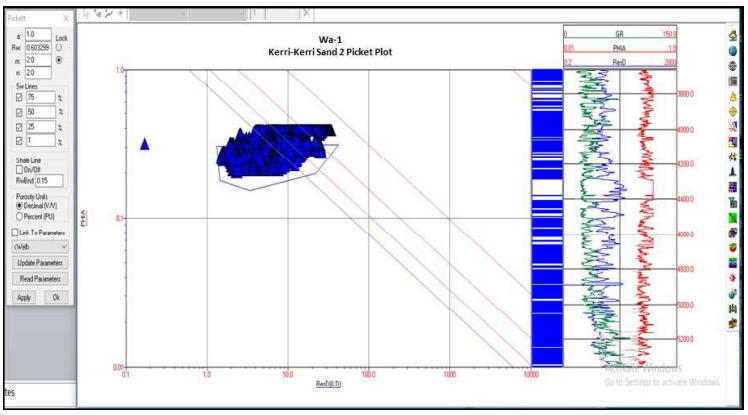



Figure 6: Picket plots of Kerr-Kerri sand-1 in Wa-1 well, $R_w$ is 0.60299Ωm

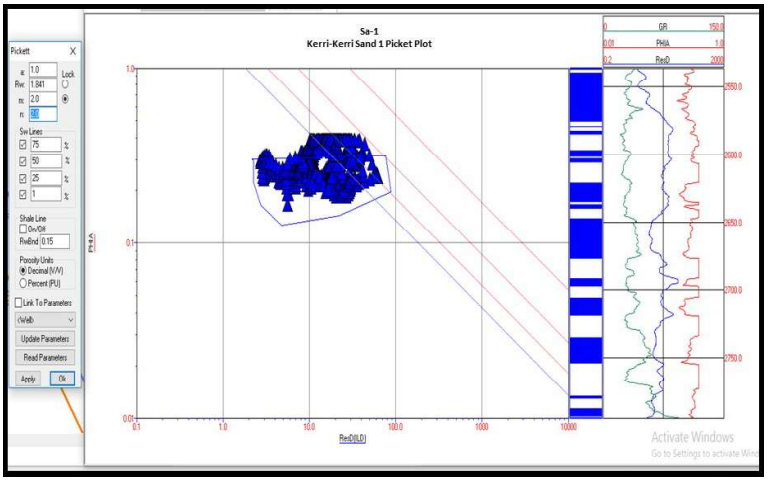



Figure 7: Picket plots of Kerr-Kerri sand-1 in Sa-1 well, $R_w$is 1.841Ωm

**Lithofacies Description**

Lithological description of Bima Sand in this study area was deciphered mainly from gamma ray log motif and a combination of other logs in complex intervals. Gamma ray logs has for long been used for identification, correlation and description of lithofacies. The application is based on the relationship between radioactivity of potassium, uranium and thorium in shale and response to gamma ray reading. Thus, the more radioactive sediment is, the more the shale content, except in cases of radioactive sand usually termed by geologists as hot sand. Chow *et al.*, (2005) used gamma ray logs of nine wells to reflect vertical profile of grain sizes

and to infer the paleo-environment of Erchungchi "A" Member. Log-derived quantitative lithofacies data based on quantitative analysis of gamma ray log motif was employed to characterize spatial and regionalized distribution of geologic facies for understanding of sub-inter-well heterogeneity in Imaemi field (Ubulom and Nwachukwu, 2014). Radioactive source is associated in varying composition, depends on depositional environment and is valuably utilized in sand and shale sedimentary facies interpretation (Nazeer *et al.,* 2016). According to the authors, it explains why normal gamma trends are used to interpret the subsurface sedimentary facies in the absence of seismic and well core data.

The tops and bases of the lithofacies picks resulted in fifteen (15) sand bodies within Bima Formation. These were named: Bima-1, Bima-2, Bima-3, Bima-3A, Bima-3B, Bima-3C, Bima-4, Bima-5, Bima-6, Bima-7, Bima-8, Bima-9, Bima-10, Bima-11 and Bima-12 (Table 2). The thickest gross sand is Bima-3, which is 287.80 m thick, encountered in Ar-1 well. The thinnest gross sand is Bima-3C, 9.70 m thick, intercepted in Da-1 well. The sand body with thickest net sand is Bima-3 (146.78 m net sand) in Ar-1 well, while the least net sand is Bima-3C (2.43 m net sand), encountered in Da-1 well. Analysis of the sand bodies revealed highest net-to-gross (NTG) of 0.89 in Bima-11 sand intercepted by Da-1 well and the least NTG of 0.16 in Bima-6 found in Ga-1 well.

The Bima sand demonstrate irregular or saw teeth gamma ray motif (Fig. 8). Irregular gamma ray curves are consistent with fluctuation of high and low readings that is, alternating shale and sand beds. This is archetypal of laminated beds of shale and sand. In the open ocean, it depicts slope or turbidites deposits, while in lacustrine setting; this motif represents periodic, alternation of moderate energy inflow, followed by a quiescent period of sediments coagulation from water.

Bima lithofacies is thinly laminated and in most part, highly undifferentiated (Fig. 8), which presents a great correlation challenge. In some part, it is difficult to pick the beginning and the end of an event. Bima-5 Sand in Ga-1 well, for instance, is 99.36 m thick, consists of 16 lenticular sand lobes and 16 shale bodies, while the sand lenses range in thickness from about 1.8 to 4.88 m and the shale from 1.22 to 11.58 m. However, the same Bima-5 Sand in Ar-1 is 399.06 m thick, made up of 11 sand lobes and 11 shale beds, with sand thicknesses varied from 1.22 to 10.06 m and shale from 0.91 to 13.11 m. In general, recorded resistivity values of the sand bodies are abnormally high. These high values may be due to a number of factors, principally lithic fragments and debris from igneous and metamorphic rocks in the region,

GALEY PROOF

sediment compaction and radioactive elements. The high resistivity values as seen in Bima-6 Sand in Ar-1 well and other sand bodies within the study area could possibly result in misrepresentation for hydrocarbon saturations in the formation by previous workers.

Table 2: Tops and Bases of Bima Sands: Gross, Net and Net-to-gross Thicknesses

| Well Name | Name of Sand | RESERVOIR TOP | | RESERVOIR BASE | | GROSS THICKNESS | NET THICKNESS | NTG |
|---|---|---|---|---|---|---|---|---|
| | | (MD) | (TVDSS) | (MD) | (TVDSS) | | | |
| | | (Ft) | (Ft) | (Ft) | (Ft) | (Ft) | (Ft) | Ratio |
| Ga-1 | Bima Sand-1 | 9523.29 | -8526.44 | 10220.47 | -9223.62 | 697.18 | 376.48 | 0.54 |
| Wa-1 | Bima Sand-1 | 13786.42 | -12831.00 | 14130.25 | -13175.00 | 344.00 | 151.36 | 0.44 |
| Da-1 | Bima Sand-1 | 12078.74 | -11130.45 | 12434.71 | -11486.42 | 355.97 | 135.27 | 0.38 |
| Ar-1 | Bima Sand-1 | 9030.18 | -8033.79 | 9314.30 | -8317.92 | 284.13 | 71.03 | 0.25 |
| Ye-1 | Bima Sand-1 | 8926.51 | -7930.12 | 9289.04 | -8292.65 | 362.53 | 221.14 | 0.61 |
| Ga-1 | Bima Sand-2 | 10252.30 | -9255.45 | 11088.58 | -10091.73 | 836.28 | 526.86 | 0.63 |
| Wa-1 | Bima Sand-2 | 14199.47 | -13244.00 | 14503.94 | -13549.00 | 305.00 | | |
| Da-1 | Bima Sand-2 | 12637.79 | -11689.50 | 12896.33 | -11948.04 | 258.54 | 121.51 | 0.47 |
| Ar-1 | Bima Sand-2 | 9524.93 | -8528.54 | 10089.24 | -9092.85 | 564.31 | 197.51 | 0.35 |
| Ye-1 | Bima Sand-2 | 9476.71 | -8480.32 | 9849.41 | -8853.02 | 372.70 | 141.63 | 0.38 |
| Ga-1 | Bima Sand-3 | 11125.98 | -10129.13 | 11298.23 | -10301.38 | 172.25 | 68.90 | 0.40 |
| Ga-1 | Bima Sand-3A | 11502.30 | -10505.45 | 11851.05 | -10854.20 | 348.75 | 212.74 | 0.61 |
| Ga-1 | Bima Sand-3B | 11881.56 | -10884.71 | 11967.85 | -10971.00 | 86.29 | 21.57 | 0.25 |
| Wa-1 | Bima Sand-3 | 15054.13 | -14099.00 | 15147.97 | -14193.00 | 94.00 | 40.42 | 0.43 |
| Wa-1 | Bima Sand-3A | 15185.37 | -14230.00 | 15232.61 | -14277.00 | 47.00 | 29.14 | 0.62 |
| Wa-1 | Bima Sand-3B | 15258.86 | -14304.00 | 15327.10 | -14372.00 | 68.00 | 34.68 | 0.51 |
| Wa-1 | Bima Sand-3C | 15345.14 | -14390.00 | 15391.08 | -14436.00 | 46.00 | 28.52 | 0.62 |
| Da-1 | Bima Sand-3 | 13296.92 | -12348.63 | 13334.65 | -12386.36 | 37.73 | 15.47 | 0.41 |
| Da-1 | Bima Sand-3A | 13402.89 | -12454.60 | 13438.98 | -12490.69 | 36.09 | 19.49 | 0.54 |
| Da-1 | Bima Sand-3B | 13530.84 | -12582.55 | 13576.44 | -12628.15 | 45.60 | 20.06 | 0.44 |
| Da-1 | Bima Sand-3C | 13639.11 | -12690.82 | 13670.93 | -12722.64 | 31.82 | 7.96 | 0.25 |
| Ar-1 | Bima Sand-3 | 10393.70 | -9397.31 | 11337.93 | -10341.54 | 944.23 | 481.56 | 0.51 |
| Ar-1 | Bima Sand-3A | 12133.86 | -11137.47 | 12605.97 | -11609.58 | 472.11 | 259.66 | 0.55 |
| Ar-1 | Bima Sand-3B | 12651.90 | -11655.51 | 13110.24 | -12113.85 | 458.34 | 187.92 | 0.41 |
| Ar-1 | Bima Sand-3C | 13182.42 | -12186.03 | 13221.46 | -12225.07 | 39.04 | 28.50 | 0.73 |
| Ye-1 | Bima Sand-3 | 10328.74 | -9332.35 | 10507.87 | -9511.48 | 179.13 | 60.90 | 0.34 |
| Ga-1 | Bima Sand-4 | 12860.56 | -11863.71 | 13207.68 | -12210.83 | 347.12 | 83.31 | 0.24 |
| Da-1 | Bima Sand-4 | 13768.70 | -12820.41 | 13806.43 | -12858.14 | 37.73 | 23.02 | 0.61 |
| Ar-1 | Bima Sand-4 | 13304.79 | -12308.40 | 13432.42 | -12436.03 | 127.63 | 66.37 | 0.52 |
| Ga-1 | Bima Sand-5 | 13325.79 | -12328.94 | 13654.20 | -12657.35 | 328.41 | 75.53 | 0.23 |
| Da-1 | Bima Sand-5 | 14122.05 | -13173.76 | 14232.28 | -13283.99 | 110.23 | 51.81 | 0.47 |
| Ar-1 | Bima Sand-5 | 13474.08 | -12477.69 | 13801.84 | -12805.45 | 327.76 | 144.21 | 0.44 |
| Ga-1 | Bima Sand-6 | 13853.67 | -12856.83 | 14335.63 | -13338.78 | 481.95 | 77.11 | 0.16 |
| Da-1 | Bima Sand-6 | 14359.25 | -13410.96 | 14692.58 | -13744.29 | 333.33 | 143.33 | 0.43 |
| Ar-1 | Bima Sand-6 | 13992.13 | -12995.74 | 14477.03 | -13480.64 | 484.90 | 252.15 | 0.52 |
| Ga-1 | Bima Sand-7 | 14428.48 | -13431.63 | 14621.72 | -13624.87 | 193.24 | 57.97 | 0.30 |
| Da-1 | Bima Sand-7 | 14744.75 | -13796.46 | 14976.05 | -14027.76 | 231.30 | 85.58 | 0.37 |
| Ar-1 | Bima Sand-7 | 14532.48 | -13536.09 | 14704.72 | -13708.33 | 172.24 | 63.73 | 0.37 |
| Ga-1 | Bima Sand-8 | 14647.97 | -13651.12 | 14785.76 | -13788.91 | 137.79 | 57.87 | 0.42 |
| Da-1 | Bima Sand-8 | 15017.72 | -14069.43 | 15182.42 | -14234.13 | 164.70 | 121.88 | 0.74 |
| Ar-1 | Bima Sand-8 | 14740.81 | -13744.42 | 14931.10 | -13934.71 | 190.29 | 72.31 | 0.38 |
| Ga-1 | Bima Sand-9 | 14816.27 | -13819.42 | 15045.28 | -14048.43 | 229.01 | 57.25 | 0.25 |
| Da-1 | Bima Sand-9 | 15213.58 | -14265.29 | 15346.79 | -14398.50 | 133.21 | 30.64 | 0.23 |
| Ar-1 | Bima Sand-9 | 15035.11 | -14038.72 | 15242.13 | -14245.74 | 207.02 | 74.53 | 0.36 |
| Da-1 | Bima Sand-10 | 15405.18 | -14456.89 | 15553.15 | -14604.86 | 147.97 | 108.02 | 0.73 |
| Da-1 | Bima Sand-11 | 15630.25 | -14681.96 | 15942.58 | -14994.29 | 312.33 | 277.97 | 0.89 |
| Da-1 | Bima Sand-12 | 16009.84 | -15061.55 | 16370.41 | -15422.12 | 360.57 | 194.71 | 0.54 |

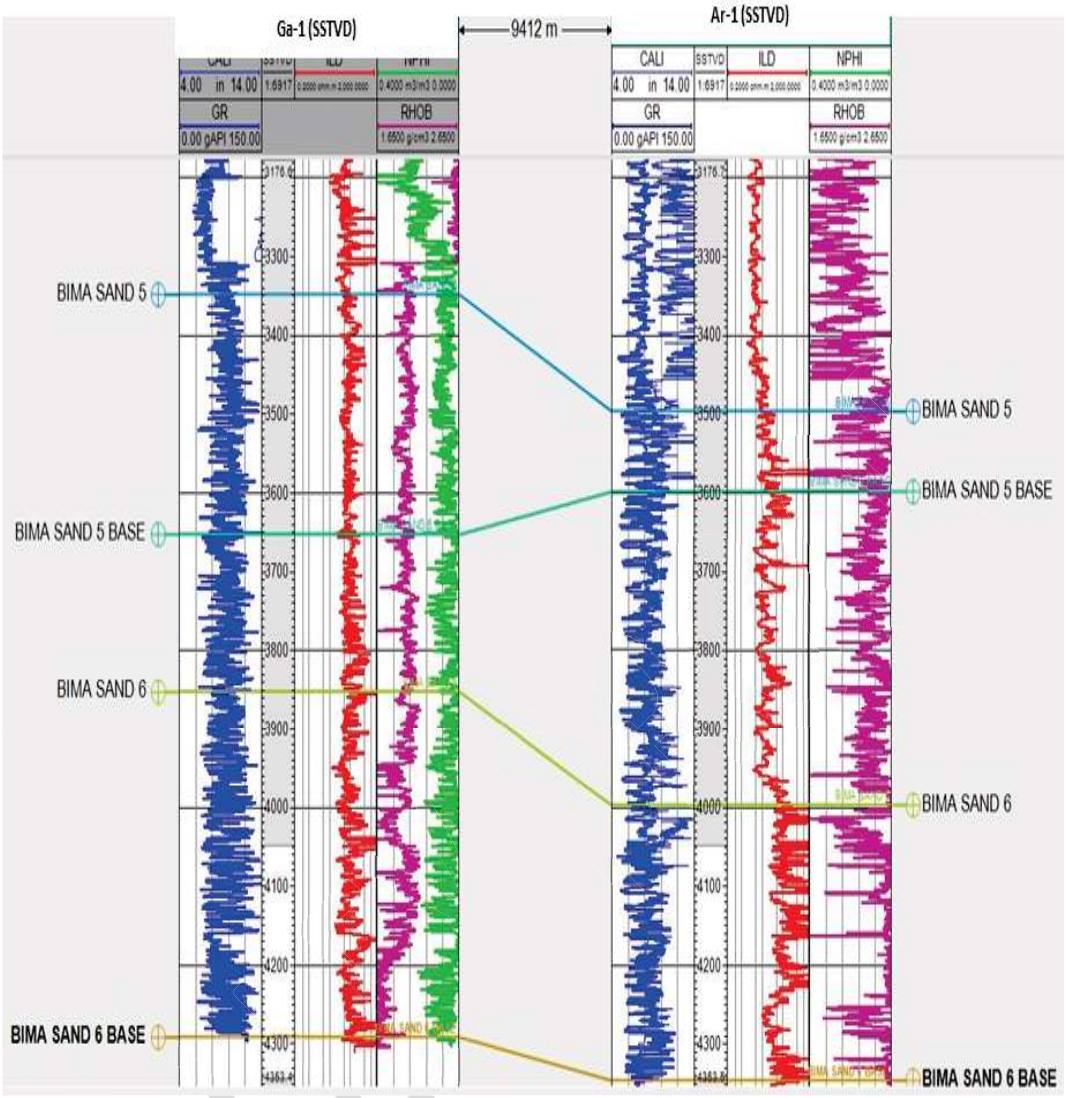



Figure 8: Serrated or Saw Teeth Gamma Ray Motif of Bima Sand, Showing alternation of Shale and Sand Lenses in Ga-1 and Ar-1 wells

**Estimation of Petrophysical Properties**

The shale volumes in Bima Sand are variable, with the least volume, 26% shale observed in Bima Sand-8 in Da-1 well depicting cleanest sand, while 88% was recorded in Bima Sand-4 in Ga-1 well. Similarly, total porosity in Bima Sand varies from field average maximum 39% in Bima Sand-8 intersected in Da-1 well to minimum 0.06 % recorded in Bima Sand-3A in Da-1 well. Effective porosity values are generally low to moderate, with field averages of 2% minimum and 24% maximum within Bima Sand 3A and Bima Sand-8 in Da-1 well and also in Bima Sand-2 of Ga-1 well. The variable porosity values are attributed in this study to compaction, diagenetic changes and mineralization within the pore spaces. Bima Sand has

low to moderate field average permeability values, which range from as low as 0.03 mD in Bima Sand-1 encountered in Ar-1 well to high value of 319 mD interpreted in Bima Sand-2 found in Ga-1 well. The Tixier (1949) and Timur (1968) methods were used to evaluate permeability values in the study area. It was discovered that the two methods give very close permeability values in all the sand studied. However, slightly higher values were given by Timur (1968) method. The highest field average hydrocarbon saturation value of 66% was recorded in Bima Sand-12 within Da-1 well, while lowest field average value, 51% was noted in Bima- Sand-1 encountered in Ga-1 well (Table 3).

Hydrocarbon saturation in the thin lenticular sand bodies also varied from 40.00 to 78.00%. It was encountered in three intervals in Ga-1, four intervals in Da-1, two intervals in Ar-1, and one interval in Ye-1. Ga-1 well encountered 30.78 m thick of hydrocarbon column in 14 thin sand lobes in Bima Sand-1, with thicknesses from 0.6 to 5.8 m and average saturation of 51.00%, while, Bima Sand-2 intercepted 45.11 m thick of hydrocarbon column within 12 thin sand lobes with average saturation of 61.00% and Bima Sand-9 has 6.3 m column in 4 thin sand lobes. Da-1 has hydrocarbon in Bima Sand-8 (5.3 m, $S_h$ of 0.58% in 5 sand lobes), Bima Sand-10 (13.5 m, $S_h$ of 52.00% in 6 sand lobes), Bima Sand-11 (6.2 m, $S_h$ of 58.00% in 2 sand lobes) and Bima Sand-12 (16.5 m, $S_h$ of 66% in 6 sand lobes). In Ar-1 well, hydrocarbon occur in Bima Sand-3 (2.4 m column, $S_h$ of 48% in a sand lobe) and Bima Sand-9 (6.0 m, $S_h$ of 58% in a sand lobe). Ye-1 well only intersected 0.50 m hydrocarbon in Bima Sand-1 with 78% saturation.

Intense bifurcation of Bima Sand bodies by shale layers, coupled with very thin nature of the sand beds with rather low average effective porosity and permeability make the pools of hydrocarbon deposits unattractive for commercial production. Furthermore, highly serrated sand bodies, complex reservoir geology and log responses, especially anomalous resistivity readings complicate interpretation of hydrocarbon occurrence and distribution in the basin. Anomalous resistivity log reading recorded in the field is attributed to mineralization and high ambient formation water resistivity value.

Table 3: Petrophysical Summary of Bima Reservoirs Showing Field Average Petrophysical Properties

| Well Name | Name of Sand | (TVDSS) | (TVDSS) | GROSS THICKNESS | NET THICKNESS | NTG | Vshl | PHIA | PHIE | BVW | SwA | Sh | K | KT | Pay Column | NTG PAY | NUMBER OF SAND LOBES |
|---|---|---|---|---|---|---|---|---|---|---|---|---|---|---|---|---|---|
| | | (Ft) | (Ft) | (Ft) | (Ft) | Ratio | % | % | % | % | % | % | mD | mD | (Ft) | Ratio | (Ft) |
| Ga-1 | Bima Sand-1 | -8,526.44 | -9,223.62 | 697.18 | 376.48 | 0.54 | 0.46 | 0.35 | 0.19 | 0.17 | 0.49 | 0.51 | 140.24 | 124.44 | 101.03 | 0.14 | 14.00 |
| Wa-1 | Bima Sand-1 | -12,831.00 | -13,175.00 | 344.00 | 151.36 | 0.44 | 0.56 | 0.00 | 0.00 | 0.00 | 0.00 | 0.00 | 0.00 | 0.00 | 0.00 | NIL | |
| Da-1 | Bima Sand-1 | -11,130.45 | -11,486.42 | 355.97 | 135.27 | 0.38 | 0.62 | 0.10 | 0.04 | 0.10 | 0.99 | 0.01 | 1.21 | 0.50 | 0.00 | NIL | |
| Ar-1 | Bima Sand-1 | -8,033.79 | -8,317.92 | 284.13 | 71.03 | 0.25 | 0.75 | 0.12 | 0.03 | 0.12 | 1.00 | 0.00 | 0.19 | 0.03 | 0.00 | NIL | |
| Ye-1 | Bima Sand-1 | -7,930.12 | -8,292.65 | 362.53 | 232.02 | 0.61 | 0.36 | 0.39 | 0.25 | 0.09 | 0.22 | 0.78 | 217.22 | 172.79 | 1.64 | 0.00 | 1.00 |
| Ga-1 | Bima Sand-2 | -9,255.45 | -10,091.73 | 836.28 | 526.86 | 0.63 | 0.37 | 0.38 | 0.24 | 0.15 | 0.39 | 0.61 | 304.71 | 319.49 | 148.62 | 0.18 | 12.00 |
| Wa-1 | Bima Sand-2 | -13,244.00 | -13,549.00 | 305.00 | | | | | | | | | | | | N/A | |
| Da-1 | Bima Sand-2 | -11,689.50 | -11,948.04 | 258.54 | 121.51 | 0.47 | 0.53 | 0.06 | 0.02 | 0.09 | 0.95 | 0.05 | 2.14 | 1.31 | 0.00 | NIL | |
| Ar-1 | Bima Sand-2 | -8528.54 | -9092.85 | 564.31 | 197.51 | 0.35 | 0.65 | 0.15 | 0.05 | 0.15 | 1.00 | 0.00 | 1.45 | 0.46 | 0.00 | NIL | |
| Ye-1 | Bima Sand-2 | 9476.71 | -8480.32 | 9849.41 | -8853.02 | 372.70 | 0.50 | 0.17 | 0.09 | 0.18 | 1.00 | 0.00 | 58.30 | 55.27 | 0.00 | NIL | |
| Ga-1 | Bima Sand-3 | -10,129.13 | -10,301.38 | 172.25 | 68.90 | 0.40 | 0.60 | 0.07 | 0.03 | 0.06 | 0.96 | 0.04 | 0.33 | 0.07 | 0.00 | NIL | |
| Ga-1 | Bima Sand-3A | -10,505.45 | -10,854.20 | 348.75 | 212.74 | 0.61 | 0.39 | 0.04 | 0.02 | 0.04 | 0.97 | 0.03 | 0.44 | 0.15 | 0.00 | NIL | |
| Ga-1 | Bima Sand-3B | -10,884.71 | -10,971.00 | 86.29 | 21.57 | 0.25 | 0.75 | 0.38 | 0.10 | 0.20 | 0.53 | 0.47 | 47.76 | 40.01 | 0.00 | NIL | |
| Wa-1 | Bima Sand-3 | -14,099.00 | -14,193.00 | 94.00 | 40.42 | 0.43 | 0.57 | 0.10 | 0.04 | 0.10 | 1.00 | 0.00 | 3.23 | 1.44 | 0.00 | NIL | |
| Wa-1 | Bima Sand-3A | -14,230.00 | -14,277.00 | 47.00 | 29.14 | 0.62 | 0.38 | 0.10 | 0.06 | 0.10 | 1.00 | 0.00 | 0.64 | 0.09 | 0.00 | NIL | |
| Wa-1 | Bima Sand-3B | -14,304.00 | -14,372.00 | 68.00 | 34.68 | 0.51 | 0.49 | 0.06 | 0.03 | 0.07 | 1.00 | 0.00 | 2.62 | 1.34 | 0.00 | NIL | |
| Wa-1 | Bima Sand-3C | -14,390.00 | -14,436.00 | 46.00 | 28.52 | 0.62 | 0.38 | 0.07 | 0.03 | 0.07 | 1.00 | 0.00 | 0.04 | 0.00 | 0.00 | NIL | |
| Da-1 | Bima Sand-3 | -12,348.63 | -12,386.36 | 37.73 | 15.47 | 0.41 | 0.59 | 0.07 | 0.03 | 0.07 | 1.00 | 0.00 | 0.19 | 0.03 | 0.00 | NIL | |
| Da-1 | Bima Sand-3A | -12,454.60 | -12,490.69 | 36.09 | 19.49 | 0.54 | 0.46 | 0.05 | 0.02 | 0.05 | 1.00 | 0.00 | 0.05 | 0.00 | 0.00 | NIL | |
| Da-1 | Bima Sand-3B | -12,582.55 | -12,628.15 | 45.60 | 20.06 | 0.44 | 0.56 | 0.23 | 0.11 | 0.20 | 0.92 | 0.08 | 74.98 | 64.21 | 0.00 | NIL | |
| Da-1 | Bima Sand-3C | -12,690.82 | -12,722.64 | 31.82 | 7.95 | 0.25 | 0.75 | 0.11 | 0.03 | 0.11 | 1.00 | 0.00 | 0.06 | 0.00 | 0.00 | NIL | |
| Ar-1 | Bima Sand-3 | -9397.31 | -10341.54 | 944.23 | 453.23 | 0.51 | 0.52 | 0.32 | 0.15 | 0.15 | 0.52 | 0.48 | 39.94 | 20.18 | 7.88 | 0.01 | 1.00 |
| Ar-1 | Bima Sand-3A | -11137.47 | -11609.58 | 472.11 | 259.66 | 0.55 | 0.45 | 0.21 | 0.11 | 0.21 | 1.00 | 0.00 | 42.47 | 32.07 | 0.00 | NIL | |
| Ar-1 | Bima Sand-3B | -11655.51 | -12113.85 | 458.34 | 187.92 | 0.41 | 0.59 | 0.17 | 0.06 | 0.16 | 0.98 | 0.02 | 13.74 | 12.82 | 0.00 | NIL | |
| Ar-1 | Bima Sand-3C | -12186.03 | -12225.07 | 39.04 | 28.50 | 0.73 | 0.27 | 0.08 | 0.06 | 0.08 | 0.98 | 0.02 | 1.52 | 0.37 | 0.00 | NIL | |
| Ye-1 | Bima Sand-3 | 10328.74 | -9332.35 | 10507.87 | -9511.48 | 179.13 | 0.66 | 0.03 | 0.01 | 0.04 | 1.00 | 0.00 | 0.03 | 0.00 | 0.00 | NIL | |
| Ga-1 | Bima Sand-4 | -11863.71 | -12210.83 | 347.12 | 83.50 | 0.24 | 0.88 | 0.39 | 0.05 | 0.15 | 0.88 | 0.12 | 16.26 | 11.92 | 0.00 | NIL | |
| Da-1 | Bima Sand-4 | -12,820.41 | -12,858.14 | 37.73 | 23.02 | 0.61 | 0.39 | 0.14 | 0.08 | 0.13 | 0.97 | 0.03 | 4.39 | 1.39 | 0.00 | NIL | |
| Ar-1 | Bima Sand-4 | -12308.40 | -12436.03 | 127.63 | 66.37 | 0.52 | 0.48 | 0.15 | 0.07 | 0.15 | 0.98 | 0.02 | 34.80 | 39.84 | 0.00 | NIL | |
| Ga-1 | Bima Sand-5 | -12328.94 | -12657.35 | 328.41 | 75.44 | 0.23 | 0.86 | 0.38 | 0.05 | 0.13 | 0.86 | 0.14 | 16.51 | 10.34 | 0.00 | NIL | |
| Da-1 | Bima Sand-5 | -13,173.76 | -13,283.99 | 110.23 | 51.81 | 0.47 | 0.53 | 0.16 | 0.06 | 0.15 | 0.95 | 0.05 | 1.67 | 0.45 | 0.00 | NIL | |
| Ar-1 | Bima Sand-5 | -12477.69 | -12805.45 | 327.76 | 144.21 | 0.44 | 0.56 | 0.14 | 0.05 | 0.14 | 0.99 | 0.01 | 2.74 | 1.04 | 0.00 | NIL | |
| Ga-1 | Bima Sand-6 | -12856.83 | -13338.78 | 481.95 | 75.44 | 0.16 | 0.86 | 0.38 | 0.05 | 0.13 | 0.86 | 0.14 | 16.51 | 10.34 | 0.00 | NIL | |
| Da-1 | Bima Sand-6 | -13,410.96 | -13,744.29 | 333.33 | 143.33 | 0.43 | 0.57 | 0.09 | 0.04 | 0.08 | 0.90 | 0.10 | 1.00 | 0.31 | 0.00 | NIL | |
| Ar-1 | Bima Sand-6 | -12995.74 | -13480.64 | 484.90 | 252.15 | 0.52 | 0.48 | 0.13 | 0.06 | 0.09 | 0.83 | 0.17 | 24.49 | 26.06 | 0.00 | NIL | |
| Ga-1 | Bima Sand-7 | -13431.63 | -13624.87 | 193.24 | 57.97 | 0.30 | 0.81 | 0.37 | 0.07 | 0.15 | 0.81 | 0.19 | 21.03 | 12.78 | 0.00 | NIL | |
| Da-1 | Bima Sand-7 | -13,796.46 | -14,027.76 | 231.30 | 85.58 | 0.37 | 0.63 | 0.08 | 0.04 | 0.07 | 0.88 | 0.12 | 0.75 | 0.17 | 0.00 | NIL | |
| Ar-1 | Bima Sand-7 | -13536.09 | -13708.33 | 172.24 | 113.68 | 0.37 | 0.34 | 0.13 | 0.08 | 0.04 | 0.42 | 0.58 | 14.48 | 8.75 | 19.68 | 0.11 | 1.00 |
| Ga-1 | Bima Sand-8 | -13651.12 | -13788.91 | 137.79 | 57.97 | 0.42 | 0.74 | 0.39 | 0.10 | 0.09 | 0.74 | 0.26 | 21.96 | 11.28 | 0.00 | NIL | |
| Da-1 | Bima Sand-8 | -14,069.43 | -14,234.13 | 164.70 | 121.88 | 0.74 | 0.26 | 0.10 | 0.07 | 0.04 | 0.42 | 0.58 | 2.07 | 0.53 | 17.39 | 0.11 | 5.00 |
| Ar-1 | Bima Sand-8 | -13744.42 | -13934.71 | 190.29 | 72.31 | 0.38 | 0.62 | 0.04 | 0.02 | 0.04 | 0.95 | 0.05 | 0.04 | 0.00 | 0.00 | NIL | |
| Ga-1 | Bima Sand-9 | -13,819.42 | -14,048.43 | 229.01 | 57.97 | 0.25 | 0.39 | 0.39 | 0.24 | 0.10 | 0.39 | 0.62 | 207.66 | 170.87 | 20.68 | 0.09 | 4.00 |
| Da-1 | Bima Sand-9 | -14,265.29 | -14,398.50 | 133.21 | 30.64 | 0.23 | 0.77 | 0.09 | 0.02 | 0.07 | 0.88 | 0.12 | 0.57 | 0.20 | 0.00 | NIL | |
| Ar-1 | Bima Sand-9 | -14038.72 | -14245.74 | 207.02 | 74.53 | 0.36 | 0.64 | 0.06 | 0.02 | 0.07 | 0.98 | 0.02 | 2.08 | 1.58 | 0.00 | NIL | |
| Da-1 | Bima Sand-10 | -14,456.89 | -14,604.86 | 147.97 | 108.02 | 0.73 | 0.27 | 0.2 | 0.14 | 0.09 | 0.48 | 0.52 | 98.63 | 97.95 | 44.29 | 0.30 | 6.00 |
| Da-1 | Bima Sand-11 | -14,681.96 | -14,994.29 | 312.33 | 277.97 | 0.89 | 0.11 | 0.12 | 0.1 | 0.05 | 0.42 | 0.58 | 4.63 | 1.06 | 20.34 | 0.07 | 2.00 |
| Da-1 | Bima Sand-12 | -15,061.55 | -15,422.12 | 360.57 | 194.71 | 0.54 | 0.46 | 0.18 | 0.1 | 0.07 | 0.35 | 0.66 | 16.91 | 9.18 | 54.12 | 0.15 | 6.00 |

CHIEF

**Bima Sand Stratigraphic Location and Reservoir Petrophysics**

The Bima Sand reservoirs studied are: Di-1, Ar-1, Ga-1 and Ye-1 wells in Maiduguri sub basin (Figures. 9 and 10) and Da-1 andWa-1 wells in Baga/Lake sub-basin (Figures 11 and 12). The wells were correlated within the sub basin. Bima Formation top is shallowest in Maiduguri Sub-basin, particularly in Ye-1 well, where it was picked at -2417.1 m tvdss, while it encountered Wa-1 well at a deeper depth of -3910.89 m tvdss within Baga/Lake Sub-basin (Table 2). Da-1 well penetrated the deepest section of Bima Formation in the studied area at -4700.66 m tvdss (Figs. 10 and 12). The thickest part of the formation encountered in this study is about 1308.1 m and it was intercepted in Da-1 well, which is also the deepest well used in the study area in Baga sub-basin. Moreover, Bima Formation becomes observably more serrated to undifferentiated sand lobes in this sub-basin. Consequently, twelve (12) sand bodies were picked and named from top (Bima-1) to base (Bima-12), while 3 sub-units were named Bima-3A, Bima-3B and Bima-3C accordingly. Thus, the total sand bodies encountered were fifteen (15). Lithofacies and petrophysical variability in Bima Formation resulted in very low effective porosity and permeability values in parts of the reservoirs and this is suggestive of diagenetic footprints on the sand deposits.

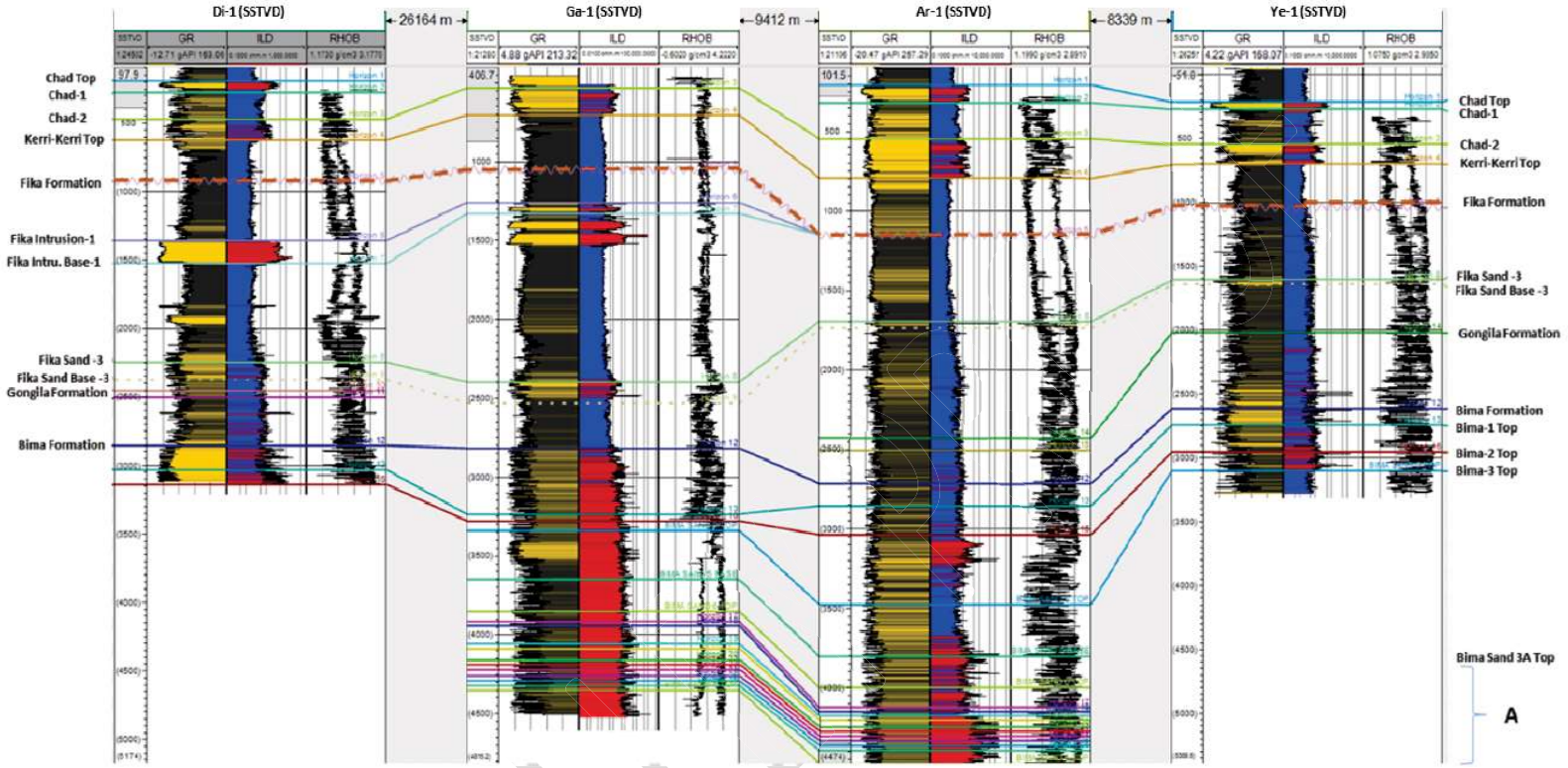



Figure 9: Stratigraphic cross section through Maiduguri Sub-basin, showing different formations in stratigraphic position through Na-1, Di-1, Ga-1, Ar-1, and Ye-1 Wells

GALLEY PROOF

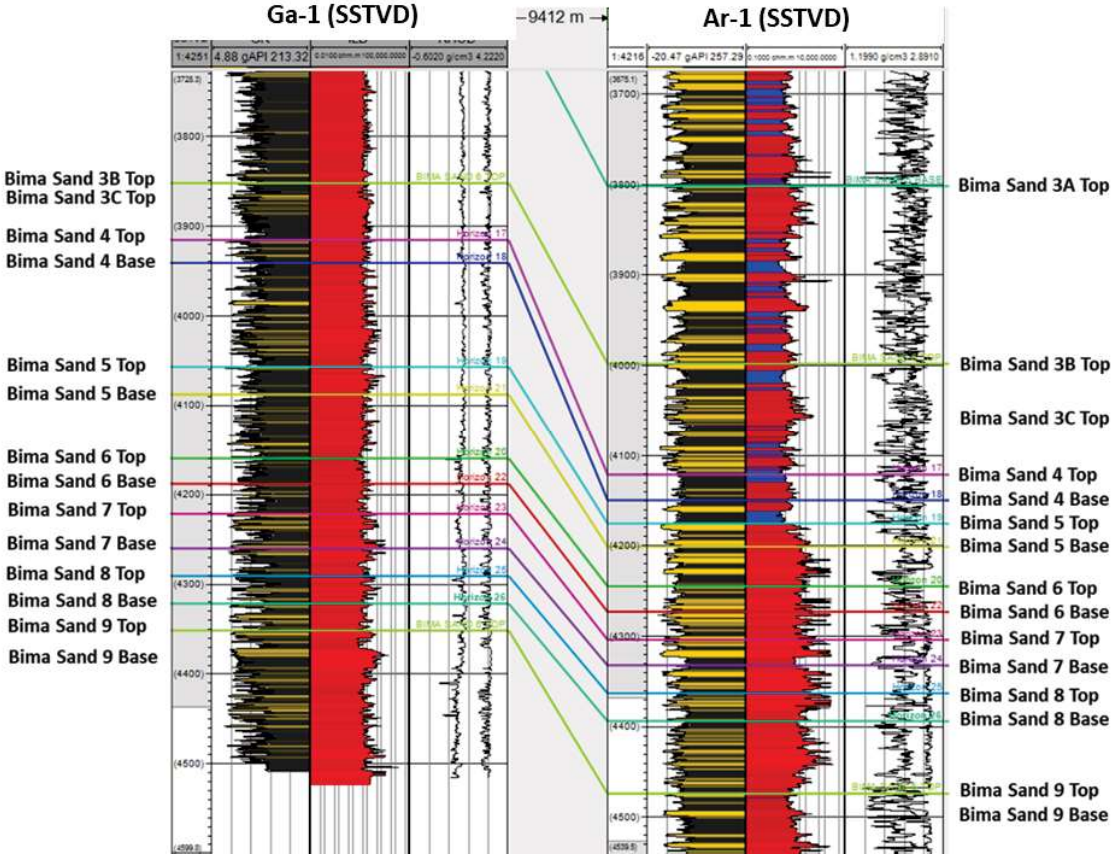



Figure 10: Enlargement of A from figure 10 showing Bima sand having centimeter-scale thin laminations

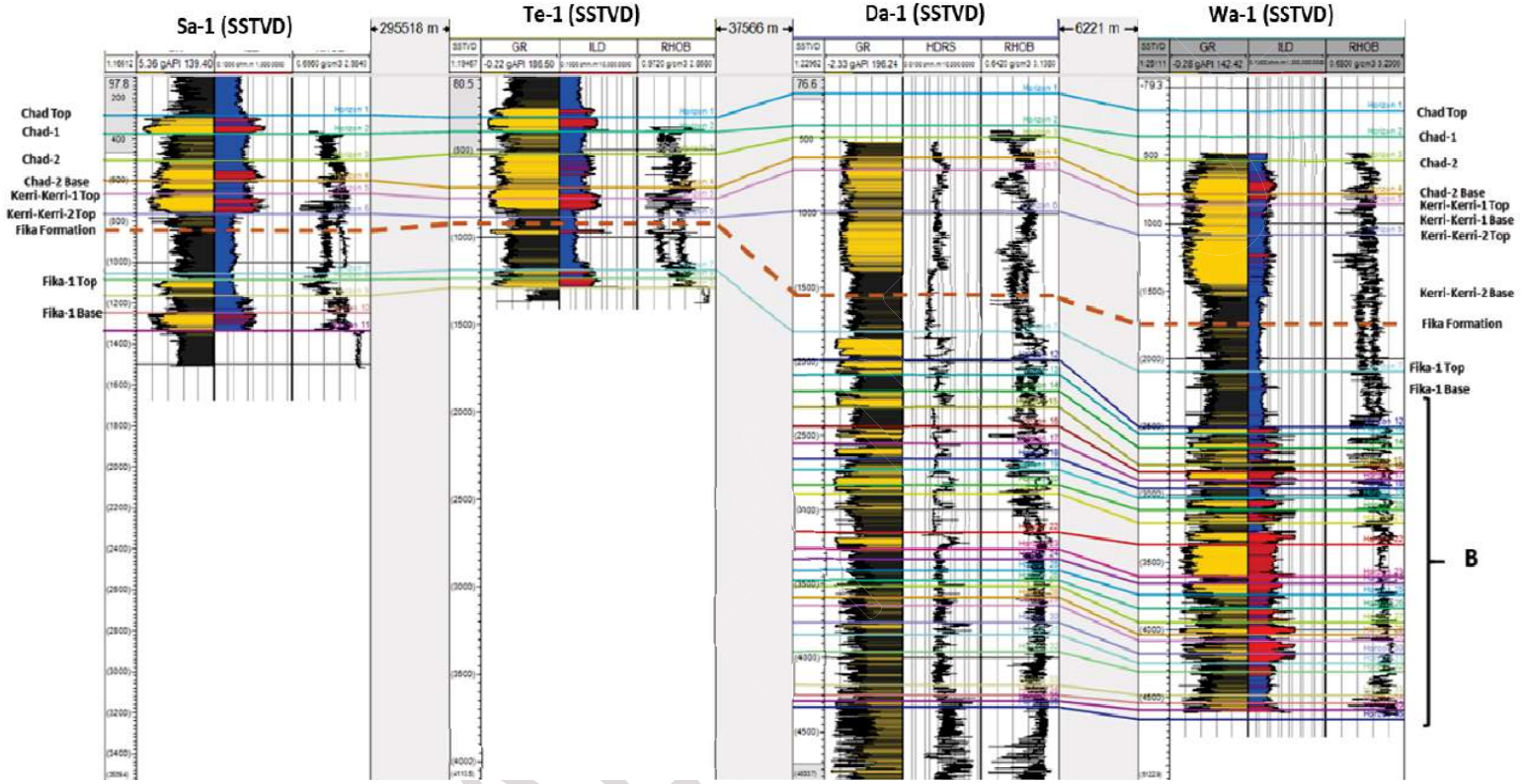



Figure 11: Baga Lake Area Geologic Cross Section through Sa-1, Te-1, Da-1 and Wa-1 wells showing different formations in stratigraphic positions

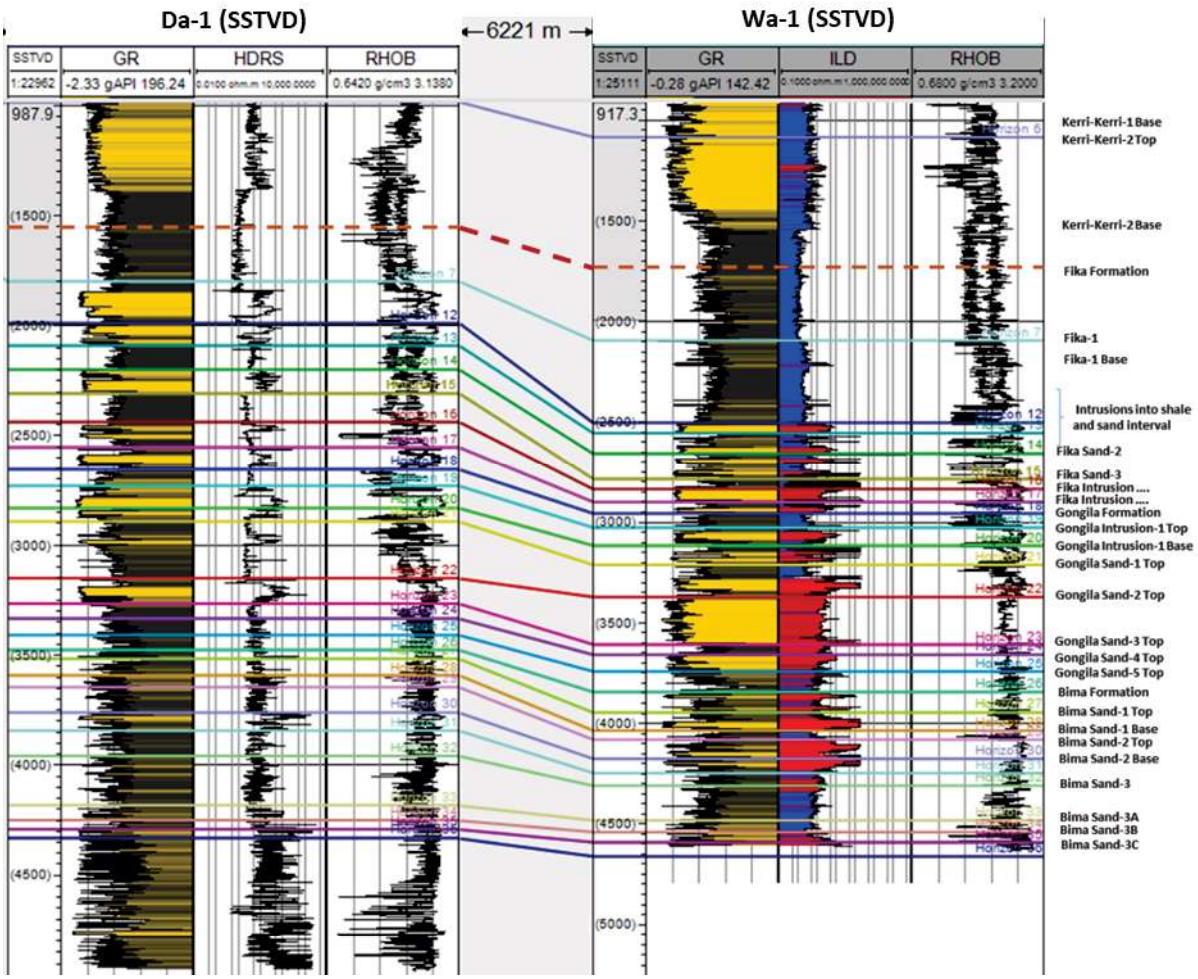



Figure 12: Enlargement of B from figure 12 showing Bima sand having centimeter-scale thin laminations.

**Depositional Environments Implications**

The depositional environment of Bima Sand is inferred in this study from the lithofacies characteristics interpreted from well logs. The peculiar heterolithic variation, dominated by thinly laminated or serrated alternation of sand and shale beds is interpreted to represent fluviolacustrine deposit. This implies that the depositional environment is related to sedimentations which occur under the influence of both streams and lake.

**Conclusions**

The Bima Formation formation is shallower in Maiduguri Area in Ye-1 well (-2417.10 m tvdss), while the thickest column (1308.10 m) was encountered in Da-1 well in the Baga Lake portion,

northeast of study area. The Formation consists of siliciclastics sand-shale alternations, as indicated by intense lamination of thin sand and shale lenticular beds.

Anomalously high resistivity log reading recorded in the field is attributed to mineralization, diagenesis and high ambient formation water resistivity value. Variability of petrophysical properties confirmed very low effective porosity and permeability values in the reservoirs due to diagenetic footprint on the sand deposits

In conclusion, Bima Sand bodies in Maiduguri sub-basin in the southwest and Baga Lake sub-basin in the northwest are similar in their lithological and petrophysical properties, as well as hydrocarbon occurrence. Hydrocarbon deposits around 40.00 to 78.00% saturation levels occur in the study area. Ga-1 well has hydrocarbon in three sand bodies, Bima-1, Bima-2 and Bima-9 respectively. Bima-1 Sand intersected 30.79 m column of hydrocarbon in 14 tiny sand lobes, while Bima-2 found 45.30 m of hydrocarbon in 12 sand lobes and 6.30 m in 4 sand lobes. In Da-1 well, hydrocarbon was encountered in Bima-8, Bima-10, Bima-11 and Bima-12 respectively, with thicknesses of 5.30 m, 13.50 m, 6.20 m and 16.50 m. These occur in 5, 6, 2 and 6 tiny sand lobes accordingly. Moreover, hydrocarbon was encountered in Bima Sand-3 (2.40 m column in a sand lobe) and Bima Sand-9 (56.0 m thick in a sand lobe) in Ar-1 well, as well as (0.5 m) in Bima Sand-1 of Ye-1. The very tin and serrated characteristic nature of the laminated sand coupled with anomalous formation water resistivity values present enormous hydrocarbon basinal assessment exploitation challenges.

The sedimentary fills are inferred to have been deposited in fluviolacustrine environment, resulting in very thinly laminated or serrated alternation of sand and shale beds lithofacies.

**References**

Adepelumi, A.A, Alao, O.A, and Kutemi T.F. 2011: Reservoir Characterization and Evaluation of depositional trend of Gombe sandstone, southern Chad basin Nigeria: Journal of Petroleum and Gas Engineering, 2 (6): 118-131.

Alalade B. & Tyson R.V. 2010: Hydrocarbon Potential of the Late Cretaceous Gongila and Fika Formations, Bornu (Chad) Basin, NE Nigeria. Journal of Petroleum Geology 33: 339-353.

GALLEY PROOF

Archie, G. E. 1942: The electrical resistivity log as an aid in determining some reservoir characteristics. Trans. Am. Inst. Mech. Eng., 146:54-62.

Avbovbo, A.A., Ayoola, E. O. and Osahon, G.A 1986: Depositional and Structural Style in Chad basin of Northeastern Nigeria. AAPG Bulletin. 70: 1787-1798.

Boboye O.A and Abimbola A.F 2009: Hydrocarbon Potential of Lithostratigraphic Units in Late Cenomanian- Early Paleocene Shale, Southwestern Chad Basin. World Applied Sciences Journal 7: 567-573

Bowers, M. C. And Fitz, D. E. 2000: A probabilistic approach to determine uncertainty in calculatedwater saturation. A paper originally presented at the SPWLA 41st Annual Logging Symposium, June 4-7.

Chow, J. J, Ming-Ching Li, Fuh S., 2005: Geophysical well log study on the paleoenvironment of the hydrocarbon producing zones in the Erchungchi Formation, Hsinyin, SW Taiwan. TAO; 16 (3): 531-43

Haruna, I. V., Dio C. J., Maunde A. and Raji A. S. 2013:Provenance and Paleoenvironmental Study of Bima Sandstone in the Upper Benue trough, N.E., Nigeria. International Research Journal of Earth Sciences 1 (2): 1-11

Genik G. J., 1992: Regional framework structure and petroleum aspects of the rift basins in Niger, Chad and Central African Republic (C.A.R.). Tectonophysics 213:169–185

Kozeny, J. 1927: Ober kapillare Leitung des Wassers in Boden: Sitzunggsbericht der Wiener Akademie, Abteilung IIa, 136:271

Larue, D. K. and Legarre, H. 2004: Flow units, connectivity, and reservoir characterization in a wave-dominated deltaic reservoir: Meren reservoir, Nigeria. AAPG Bull. 88 (3): 303–324.

Nazeer, A., Abbasi, S. A., Solangi, S. H. 2016: Sedimentary facies interpretation of Gamma Ray (GR) log as basic well logs in Central and Lower Indus Basin of Pakistan Geodesy and Geodynamics, 7 (6) 432-443.

Obiora, F. I., Yashi, J., Sani, R. O and Mondigha, E. B. 2014: Depositional Environment of Bima Sandstone In Hinna Community in Yamaltu/Deba Local Government Area Of Gombe State, Nigeria and Its Economic Importance in Construction. Int. J. Engr. Res. & Sci. & Tech.3 (2) 1-16

Olugbemiro R.O., Ligouis B. & Abaa S.I 1997: The Cretaceous series in the Chad basin, NE Nigeria: Source Rock Potential and thermal maturity. Journal of Petroleum Geology, 20: 51-68.

Opeloye, J. A., Ola, P. S., and Olabode, S. O. 2014: Possible Bornu Basin Hydrocarbon Habitat – A Review International Journal of Geosciences, 5: 983-996

Steiber, S. J. 1970: "Pulse Neutron capture log evaluation in the Louisiana Gulf Coast" SPE paper 2961, presented at the SPE Annual Meeting, Houston, October, 4-7.

Timur, A. 1968: An investigation of permeability, porosity and residual water Saturation relations for sandstone reservoirs: The Log Analyst, 9 (4): 8-17.

Tixier, M. P. 1949: Evaluation of permeability from electric log resistivity gradient. Earth Science Journal. 2: 113.

Ubulom, D. E. N. and Nwachukwu, J. I. 2014: Geostastistical Modelling of Log-Derived Quantitative Lithofacies Data, Offshore Niger Delta. NAPE Bulletin, 26 (2): 51-66

GALLEY PROOF